

Pay Attention Later: From Vector Space Diffusion to Linearithmic Spectral Phase-Locking

Alper Yıldırım  ¹ İbrahim YÜCEDAĞ  ¹

Abstract

Standard Transformers suffer from a “Semantic Alignment Tax”, a prohibitive optimization cost required to organize a chaotic initialization into a coherent geometric map via local gradient diffusion. We hypothesize that this reliance on diffusive learning creates “Catastrophic Rigidity”, rendering models unable to adapt to novel concepts without destroying their pre-trained reasoning capabilities. To isolate this phenomenon, we introduce Iterative Semantic Map Refinement (ISMР), a diagnostic protocol revealing that alignment is a fixed geometric barrier that scaling cannot solve; a 20-layer model overcomes this barrier no faster than a 1-layer model.

We introduce the Phase-Resonant Intelligent Spectral Model (PRISM). PRISM encodes semantic identity as resonant frequencies in the complex domain (\mathbb{C}^d) and replaces quadratic self-attention with linearithmic $O(N \log N)$ Gated Harmonic Convolutions. We validate PRISM on the WMT14 translation task. While the Standard Transformer maintains a slight edge in general competence on static benchmarks (23.88 vs 21.40 BLEU), it fails the “Plasticity-Stability” stress test completely. When injected with novel concepts, the Transformer suffers Catastrophic Forgetting, degrading by -10.55 BLEU points while achieving only 60% acquisition. In contrast, PRISM demonstrates *Lossless Plasticity*, achieving 96% 5-shot acquisition with negligible degradation (-0.84 BLEU). These results suggest that harmonic representations effectively decouple memory from reasoning, offering a structural solution to the plasticity-stability dilemma in real-time knowledge adaptation.

¹Department of Computer Engineering, Düzce University, Turkey. Correspondence to: Alper Yıldırım <yildirim.alper.dev@gmail.com>, İbrahim Yücedağ <ibrahimyucedag@duzce.edu.tr>.

Preprint.

1. Introduction

Effective relational reasoning prioritizes logical relationships over surface features, a capacity often attributed to strong inductive biases regarding the structure of information (Webb et al., 2024). However, effective reasoning requires a fundamental prerequisite: Semantic Geometry. A child operates on a structured mental map where concepts like “King” and “Queen” already possess meaningful proximity.

In contrast, dominant neural architectures like the Transformer (Vaswani et al., 2017) lack this pre-existing structure. Initialized with random weights, these models begin in a state of representational chaos, expending a significant portion of their compute budget just to discover a coherent semantic space.

We identify the “Semantic Alignment Tax” not as a capacity limitation, but as a structural mismatch: the inherent inefficiency of capturing non-local, harmonic semantic topology via local gradient diffusion. Based on our empirical analysis, we propose that future architectures may need to decouple representation from reasoning to eliminate this cost. We specifically explore the theoretical potential of extending the geometric logic of Rotary Position Embeddings (RoPE) (Su et al., 2024) to semantic space, modeling identity not as static coordinates, but as resonant frequencies in the complex domain.

Neuroscientific studies suggest that biological systems avoid this tax by supporting non-local computation, where functional networks emerge as harmonic waves on the connectome (Atasoy et al., 2016). Crucially, capturing these long-range interactions requires modeling dynamics with complex harmonics rather than simple diffusion (Deco et al., 2025; Naselaris et al., 2009).

We contend that current scaling strategies merely mask this tax rather than solving it. As a proof-of-concept, we employ Iterative Semantic Map Refinement (ISMР), a diagnostic methodology designed to isolate the impact of the semantic map’s quality. Our findings demonstrate that the alignment tax is a fixed geometric barrier, motivating a shift toward harmonic, signal-based representations.

2. Related Work: Fixing the Processor vs. Fixing the Representation

The struggle for data efficiency in Transformers has led to two distinct philosophical approaches: (1) building more complex processors (i.e., new attention mechanisms) to untangle messy information, and (2) improving the representations that the processor acts on.

2.1. Architectural Inductive Biases: The “Processor” Fix

A prominent line of research (Altabaa et al., 2024; Webb et al., 2024) argues that Transformers lack a “relational bottleneck.” This theory posits that the brain achieves efficiency by architecturally separating abstract reasoning from raw sensory features.

The first implementation of this, the *Abstractor* (Altabaa et al., 2024), was a subtractive architecture. It forced a “hard bottleneck” by compressing inputs into abstract symbols and discarding token-level features. This seems highly effective for *purely relational* toy tasks (e.g., “Object Sorting”) where the goal is to identify a logical rule regardless of the object’s identity. However, as the authors note, this “hard bottleneck” is detrimental for *partially-relational* tasks like NMT, where specific token identities (e.g., “King”) are semantically essential and cannot be discarded.

This insight led to an important architectural evolution: the *Dual Attention Transformer* (DAT) (Altabaa & Lafferty, 2025). DAT is an additive architecture that abandons the hard bottleneck, instead running a standard “sensory” Transformer in parallel with a new, complex “relational attention” processor.

The Benchmark Mismatch. While DAT represents a significant engineering improvement, its evaluation relies heavily on the “Relational Games” benchmark (DAT, Fig. 2). We argue that success on these benchmarks—which test *abstract logic* (e.g., symmetry detection)—may not be a transferable metric for an architecture’s suitability for *semantic geometry* tasks like language.

This distinction is evidenced by the authors’ own language ablation (Appendix D.3, Fig. 12). When testing their original, simpler “Abstractor” (RCA) mechanism within the DAT architecture on language modeling, it performed only on par with a standard Transformer. This suggests that the impressive gains of DAT on language stem from its new, highly complex “Relational Attention” (RA) implementation and added tunability, rather than the original “bottleneck” principle itself. In our view, this body of work represents a “Processor-First” fix: attempting to build a more complex engine to navigate a map that is still fundamentally disordered.

2.2. Representation-First Approaches: The “Representation” Fix

Our work explores a complementary thesis: that for tasks dependent on semantic geometry, the fundamental bottleneck is not the processor’s reasoning ability, but the structural integrity of the map it operates on. Several existing methods implicitly support this view.

Pre-trained embeddings are the most common strategy. As shown by Qi et al. (Qi et al., 2018), initializing with pre-trained vectors is particularly critical in low-resource scenarios, yielding gains of up to 20 BLEU points. This effectively allows the model to “pre-pay” the alignment tax. However, this strategy is mechanically fragile; Kim et al. (Kim et al., 2024) demonstrate that without strict standardization, pre-trained embeddings introduce statistical mismatches that can destroy sequence information.

Rotary Position Embeddings (RoPE) (Su et al., 2024) offer a more fundamental precedent for our position. RoPE demonstrated that positional relationships are best encoded not by additive perturbations (which require learning), but by rotating the vector in the complex plane ($e^{im\theta}$). This multiplicative interaction allows relative distance to be preserved automatically. We argue that this success is not accidental; it is evidence that relational properties—whether positional or semantic—require complex harmonic representations rather than static Euclidean coordinates.

Embedding Prediction and Disentanglement (Hirasawa & Komachi, 2019; Kumar & Tsvetkov, 2019; Li et al., 2022) alter the learning objective to predict continuous vectors or force latent variables into specific statistical priors (e.g., Gaussian mixtures). While Li et al. (Li et al., 2022) successfully demonstrate that structured priors can aid low-resource generation, we contend that these methods essentially “patch” the statistical distribution without correcting the underlying optimization dynamics. They still rely on the encoder to learn the mapping via local diffusion, leaving the fundamental “Alignment Tax” in place.

3. Diagnostic Methodology: Isolating the Tax (ISMR)

Our central goal is to empirically test the existence and impact of the semantic alignment tax. To do this, we first formalize our hypothesis and the specific, testable predictions that follow from it. We then describe our experimental design, Iterative Semantic Map Refinement (ISMR), which was created specifically to isolate the variable of interest: the quality of the semantic map.

3.1. Formal Hypothesis and Predictions

Formally, we hypothesize that the initial optimization window, specifically the “construction phase” ($t < 400$), is constrained by a fixed geometric barrier rather than limited model capacity. We posit that the optimizer must first organize the random initialization into a topologically coherent manifold before effective reasoning can occur. This hypothesis implies three distinct, falsifiable consequences for early training dynamics.

First, if the tax is a fixed geometric entry fee located at the input interface, we predict invariant alignment latency. A massive 20-layer model should be unable to leverage its additional depth to resolve the initial geometric disorder any faster than a 1-layer model, suggesting that reasoning capacity is irrelevant until the semantic map is established.

Second, we predict that this bottleneck is strictly topological, not statistical. A model initialized with a map that is statistically perfect (correct mean and variance) but geometrically shuffled should perform no better than a random initialization. This would suggest that the optimizer requires specific relational coordinates, not just a stable distribution.

Finally, we predict that this construction phase is mechanically distinct from reasoning refinement. By injecting a pre-aligned map via ISMR, we expect to eliminate the warm-up latency entirely. This should convert the optimization trajectory from a sigmoidal construction curve to an immediate logarithmic refinement curve starting at Step 0.

3.2. Experimental Design: Isolating the Semantic Map with ISMR

To test these predictions, we designed the Iterative Semantic Map Refinement (ISMR) procedure (Figure 1). This protocol explicitly separates the learning of the semantic map (embedding weights) from the reasoning modules (encoder/decoder), allowing us to isolate the specific computational cost of geometric alignment. Crucially, this is achieved strictly within the limits of the target dataset, avoiding the confounding variables introduced by external pre-trained embeddings.

We operationalize this isolation via the following four-step pipeline:

Iteration 1 (Baseline Training): A standard Transformer is initialized with random weights and trained for N steps to establish a stable embedding space.

Map Extraction: At step N , we extract the learned embedding matrix, termed the “semantic map” E_1 , representing a converged geometry.

Model Re-initialization: We instantiate a new model and load E_1 . Critically, all reasoning parameters (encoder, decoder) are re-initialized to random to ensure that no logical rules are inherited.

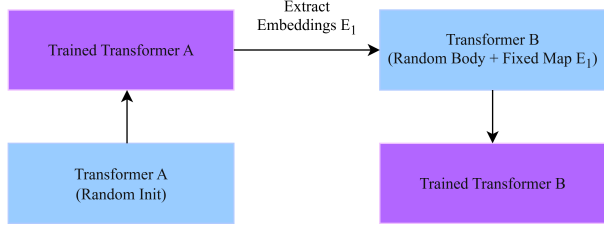


Figure 1. Diagram of the ISMR diagnostic procedure.

Refinement Training: This new model is trained for N steps, allowing us to observe the pure optimization velocity of a reasoner unburdened by map construction.

3.3. Implementation Details

Dataset Rationale: We utilize the Multi30k German-to-English (de-en) dataset (Elliott et al., 2016). This dataset was selected specifically to function as a “stress test” for geometric initialization for two reasons. First, the $\sim 29,000$ sample size creates a data-scarce environment where the model cannot rely on massive gradient updates to overcome a poor initialization. This prevents the “Alignment Tax” from being masked by scale, allowing us to inspect early training dynamics and the initial learning curve with high resolution. Second, the German-English pair presents a non-trivial embedding alignment challenge due to distinct morphological structures, ensuring that the task remains geometrically demanding despite the dataset’s small size.

Model Architectures: To isolate the “semantic tax” from the “optimization tax” of deep networks, we use two Transformer architectures, both sharing a d_{model} of 512, 8 attention heads, and a d_{ff} of 2048. Both models use a stable Pre-LayerNorm (Pre-LN) configuration (Nguyen & Salazar, 2019) and share the same $\sim 58k$ token vocabulary derived from the OPUS-MT tokenizer (Tiedemann & Thottingal, 2020).

1. “Deep” (20-Layer): A 20-encoder and 20-decoder layer model with $\sim 176.9M$ total parameters. In this architecture, the $\sim 25.7M$ parameters of the shared embedding map constitute $\sim 14.5\%$ of the model’s total parameters. The “reasoner” (the 40 layers) makes up the other $\sim 85.5\%$.

2. “Wide” (1-Layer): A 1-encoder and 1-decoder layer model with $\sim 37.2M$ total parameters. The embedding map is identical ($\sim 25.7M$ params). Here, the map constitutes $\sim 69.2\%$ of the model’s total parameters, while the “reasoner” (the 2 layers) makes up only $\sim 30.8\%$.

This “Deep” vs. “Wide” setup provides the perfect testbed. We can now measure the impact of the semantic map on two architectures where its relative parameter cost is vastly different (14.5% vs 69.2%).

Training and Evaluation: All experiments were run for 4 independent seeds (115, 116, 117, 118) and trained for 3,600 steps. We use the AdamW optimizer with a cosine learning rate schedule and a peak learning rate of 1e-4. Performance is evaluated with the BLEU score at steps [200, 400, 800, 1200, 2000, 2800, 3600]. All plots show the average of the 4 seeds, with 95% confidence intervals. To ensure stability we apply global gradient clipping with a max norm of 1.0.

Warmup Step Rationale: Our central hypothesis concerns the high cost of the alignment tax in the initial phase of training. To create the most direct test for this, we intentionally chose a very short, unified warmup of 120 steps for all experimental runs. By demonstrating that ISMR excels even under this aggressive, “fast start” schedule, we provide strong evidence that it directly mitigates the need for a prolonged and inefficient initial alignment phase.

Batching Strategy: We employ a pre-batched dataset derived from the 30k samples, which allows for highly efficient, deterministic training runs and removes any noise from dynamic batching strategies.

4. Diagnostic Results: The Invariance of the Tax

We present our findings in three parts, designed to isolate the mechanics of alignment from the confounders of external pre-training. First, we use a “Deep” model to quantify the Semantic Alignment Tax in a controlled environment, demonstrating that map formation is a distinct structural burden. Second, we employ a “Wide” model as a rigorous control to test structural invariance. By contrasting the “Deep” architecture (where the map constitutes only $\sim 14.5\%$ of parameters) against the “Wide” architecture (where the map dominates at $\sim 69.2\%$), we reveal a critical insight: the cost of alignment remains invariant (Figure 4). This suggests that the Tax is a fixed geometric entry fee, independent of the model’s depth or reasoning capacity. Finally, we present robustness checks to confirm that this barrier is a fundamental property of the optimization landscape, not a statistical artifact of initialization.

4.1. The “Deep” Model: Diagnosing a Massive Semantic Tax

Our primary experiment uses a 20-layer “Deep” Transformer, where the semantic map constitutes only $\sim 14.5\%$ of the total parameters. Figure 2 visualizes the cost of alignment.

The Baseline (Iter 1) curve reveals the significant computational overhead of co-adapting the map and the reasoner, which we identify as structural waste. As shown in Figure 2, the baseline model suffers from a prolonged “cold start,” struggling to organize the semantic space before effective

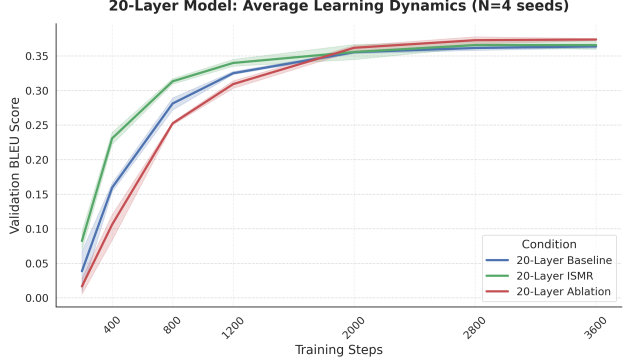


Figure 2. 20-Layer Model Average Learning Dynamics.

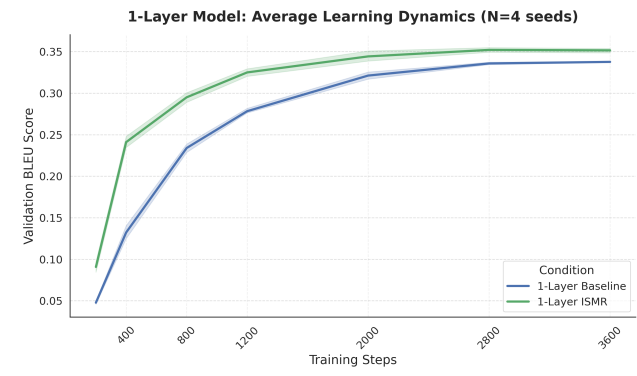


Figure 3. 1-Layer Model Average Learning Dynamics

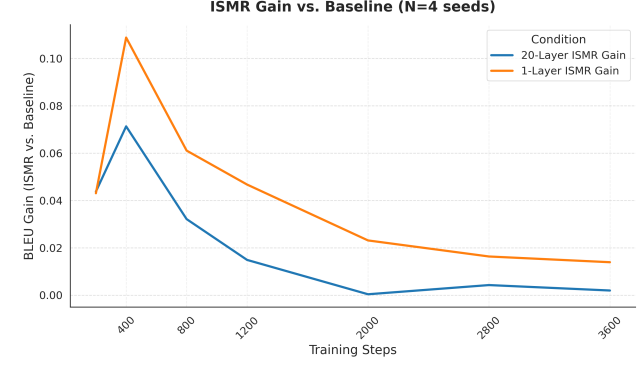


Figure 4. ISMR Gain vs. Baseline.

reasoning can begin. In sharp contrast, the ISMR model (Iter 2) bypasses this construction phase entirely. Initialized with a coherent map, it exhibits an immediate, steep performance ascent, effectively converting a chaotic initialization into a stable “warm start.” The persistent lag between these two curves is not merely a delay; it is the visualized *Semantic Alignment Tax*—the compute budget wasted on constructing geometry rather than learning the task.

Crucially, the Ablation (Shuffled) run (Figure 2, red curve) provides evidence that this bottleneck is topological, not statistical. Despite possessing the *exact same* learned statistical distribution (mean, variance, magnitude) as the ISMR

map, the Ablation model suffers a catastrophic start. This suggests that having “good statistics” is insufficient. The optimizer does not just need a well-distributed embedding space; it needs a *topologically coherent* one. The fact that the “Shuffled” map performs worse than random initialization confirms that geometric incoherence is the dominant constraint in the early optimization landscape.

4.2. The “Wide” Model: A Fixed Geometric Entry Fee

A skeptic might argue that the alignment tax is merely a symptom of deep and complex optimization landscapes, or perhaps a “depth penalty.” To test this, we performed an architectural inversion. We repeated the experiment with a 1-layer “Wide” model where the semantic map dominates the parameter count at 69.2%. This completely reverses the ratio of the “Deep” model where the map is only 14.5% of the total parameters.

The learning dynamics of this inverted architecture are visualized in Figure 3. Despite the massive reduction in depth, the Baseline model still exhibits the characteristic lag required to organize the embedding space.

The result is striking in its consistency, suggesting that this tax is an architecturally invariant entry fee. As shown in Figure 4, the initial “jump start” provided by ISMR is magnitude-invariant across architectures. Despite the vast difference in parameter count, both the Deep and Wide models exhibit a nearly identical performance gain at the onset of training. This implies that the cost of alignment is a fixed geometric barrier independent of the model’s depth or reasoning capacity.

This confirms that geometric alignment dictates learning velocity. The fact that the 20-layer model (with massive reasoning capacity) and the 1-layer model (with minimal capacity) receive the *exact same* initial boost suggests that the bottleneck is located strictly at the *input interface*. The “Deep” model cannot use its extra layers to overcome the bad geometry any faster than the “Wide” model. This implies that if we prioritize *Representation-First* initialization to secure this geometric stability early, we unlock a fixed acceleration bonus that applies regardless of the model’s depth.

4.3. Robustness Check: A Mechanically Different Problem

Finally, we performed a stress test to verify that the alignment tax dictates the optimization regime. We repeated our experiments using an aggressive learning rate of 8e-4. This high-energy setting is typically required for standard models to escape the initial chaotic plateau.

The results reveal a distinct phase shift in the optimization landscape. The aggressive rate improved the Baseline model

Table 1. Final Test BLEU Scores.

GROUP	MEAN	STD	COUNT
20-LAYER BASELINE	36.3867	0.4311	4
20-LAYER ISMR	36.8647	0.4292	4
20-LAYER ABLATION	36.6644	0.2567	4
1-LAYER BASELINE	33.9155	0.2588	4
1-LAYER ISMR	34.9642	0.2888	4

because the high variance helped it construct the map from scratch. Conversely, this same rate degraded the model initialized with the pre-aligned map. This dissociation suggests that a geometrically aligned model behaves as if it were in a “Refinement Phase” from step zero. In contrast, the baseline is trapped in a high-variance “Construction Phase” that requires large gradient updates. This confirms that the Semantic Alignment Tax constitutes a distinct stage of training with unique optimization requirements.

4.4. Disentangling Statistics vs. Geometry

While the learning curves (Fig. 2) demonstrate the massive *efficiency* cost of the Semantic Tax, the final test scores (Table 1) allow us to mechanically dissect the components of that cost.

The results reveal two distinct inductive biases:

- **The Statistical Bias:** The Ablation model (36.66 BLEU) outperforms the Baseline (36.38 BLEU). Since the Ablation uses a shuffled map, it lacks geometry but possesses the correct statistical distribution of a converged map. This confirms that standard random initialization is statistically suboptimal.
- **The Geometric Bias:** Crucially, the consistent performance gap (+0.20 BLEU) between the ISMR and Ablation models isolates the specific cost of geometric incoherence. Since both models share the exact same statistical properties, this residual gain is attributable solely to non-local relational geometry.

The Ceiling is not the Point. While all models eventually converge to a similar performance ceiling after 3,600 steps, this convergence is an expected artifact of the dataset size. For the purpose of diagnosing the alignment tax, the final score is secondary. The critical insight is the trajectory. The Baseline requires thousands of additional steps just to reconstruct the geometry that the pre-aligned map provided at step zero. The table suggests that fixing the statistics helps, but fixing the geometry is the fundamental requirement for efficient learning.

5. Theoretical Motivation

Critically, standard pre-training is not a solution to the mechanism of alignment; it is merely a way to “pre-pay” the tax using massive external resources. ISMR allows us to strip away the external data advantage and isolate the geometric alignment cost. Our finding that the “Deep” (20-layer) and “Wide” (1-layer) models suffer an identical initialization penalty suggests that this is a fundamental structural flaw in how Transformers build maps, not a capacity issue that can simply be scaled away.

5.1. The Sculptor’s Dilemma: Why Hypernetworks Fail

A logical engineering solution to this problem would be to use a Hypernetwork to predict a new token’s embedding vector directly from its definition, effectively automating the placement process. However, attempts to do so face a fundamental stability challenge (Chang et al., 2020).

We argue that this failure is a predictable consequence of the functional hierarchy of the Transformer. As shown by **Tenney et al.** (Tenney et al., 2019), Transformer layers process information in a strict sequence: early layers (0-4) focus on coarse local syntax, while semantic relations emerge only in the deepest layers. This creates a destructive mismatch we term the “Sculptor’s Dilemma.”

The early layers function as coarse feature extractors, optimized to ingest raw, high-variance input and extract local syntax. We characterize this as the “Aggressive Dimensional Collapse” effect: these layers apply high-magnitude transformations designed to reduce entropy. By injecting a semantically converged embedding (the “finished statue”) at Layer 0, we expose it to this destructive processing. Because the early layers are optimized to refine noise rather than preserve fine-grained structure, they effectively destabilize the delicate semantic geometry before it can reach the reasoning layers.

5.2. The Relational Map: Biological vs. Artificial

This fragility points to a deeper issue: the mismatch between the static nature of vector embeddings and the relational nature of meaning. Work by **Naselaris et al.** (Naselaris et al., 2009) demonstrates that biological systems represent concepts as positions within a distributed, relational map. In such a geometry, the introduction of a new concept (e.g., “Apple Inc.”) creates a geometric tension that necessitates a global relaxation of the manifold.

Standard optimization methods like SGD attempt to simulate this global re-balancing through thousands of local updates (diffusion). This is the Semantic Alignment Tax: the computational cost of simulating a non-local, elastic adjustment using only local, rigid updates.

5.3. The Barrier to One-Shot Learning

Consequently, the tax is not merely a training delay; it is a *barrier to one-shot acquisition*. Consider the “Long Tail” problem: a high-frequency concept grants the optimizer sufficient budget to pay the tax via diffusion. However, for a new concept appearing only once, the chaotic initialization dominates the signal because the gradients from a single exposure are insufficient to traverse the geometric distance required for alignment.

By shifting to a harmonic framework, as proposed in our Future Directions, the introduction of a new concept would function not as a local perturbation, but as a new frequency entering a chord. This would theoretically allow for rapid global integration of novel information, solving the few-shot learning problem by bypassing the destructive transformations of early diffusive layers.

6. The PRISM Architecture

We introduce the **Phase-Resonant Intelligent Spectral Model (PRISM)**, a harmonic architecture designed to eliminate the Semantic Alignment Tax. Unlike standard Transformers, which treat semantic identity as static coordinates in a vector space \mathbb{R}^d , PRISM encodes identity as resonant frequencies in the complex domain \mathbb{C}^d . This shift allows the model to replace the quadratic search of attention with the linearithmic synchronization of phase-locking.

6.1. Harmonic Embeddings: The Rotational Manifold

In a standard Euclidean embedding, a token x is represented as a static vector $v_x \in \mathbb{R}^d$. In PRISM, we redefine the embedding space as a system of oscillators. We decompose the embedding of a token at sequence position t into two distinct components: a learnable *Amplitude* (Semantics) and a fixed *Frequency* (Dynamics).

Formally, the harmonic embedding $H(x, t)$ is defined as:

$$H(x, t) = \mathcal{A}(x) \odot e^{i\omega t} \quad (1)$$

Where:

- $\mathcal{A}(x) \in \mathbb{R}^d$ is the learnable Amplitude Vector, representing the semantic “volume” of the token (e.g., the importance of the concept).
- $\omega \in \mathbb{R}^d$ is a fixed vector of Angular Frequencies, geometrically spaced to capture multi-scale dynamics.
- \odot denotes element-wise multiplication.

This formulation ensures that “position” is not an additive bias but a rotational operator. Consequently, the interaction

between two tokens depends only on their relative distance (phase difference), inherently satisfying the shift-invariance property required for sequence modeling.

6.2. Gated Harmonic Convolution (GHC)

To process these harmonic representations without destroying their phase information, we introduce the **Gated Harmonic Convolution (GHC)** layer. This layer replaces the Multi-Head Self-Attention (MHSA) mechanism found in standard architectures.

Phase-Preserving Activation (ModReLU) Standard activation functions like ReLU operate on real values and destroy phase information by strictly rectifying negative values, effectively resetting angles. To maintain wave coherence, we employ ModReLU (Arjovsky et al., 2016), which scales the magnitude while preserving the phase angle θ_z :

$$\text{ModReLU}(z) = \text{ReLU}(|z| + b) \cdot \frac{z}{|z|} \quad (2)$$

where $b \in \mathbb{R}^d$ is a learnable bias parameter.

Spectral Gating To mitigate the "vanishing phase" problem inherent in deep complex-valued networks, we introduce a learnable **Spectral Gate** g . Initialized to an open state ($\sigma(g) \approx 1.0$), this gate allows the network to selectively filter frequencies before the convolution, acting as a learnable band-pass filter. The gated signal z_{gated} is computed by concatenating the real and imaginary parts:

$$z_{gated} = z \cdot \sigma(W_{gate} [\Re(z) \parallel \Im(z)]) \quad (3)$$

Global Resonance via FFT Instead of computing pairwise attention scores with $\mathcal{O}(N^2)$ cost, PRISM computes global interactions via the Convolution Theorem. The sequence interaction is defined as a multiplication in the frequency domain:

$$Y = \mathcal{F}^{-1} (\mathcal{F}(X) \odot K) \quad (4)$$

Where \mathcal{F} denotes the Fast Fourier Transform (FFT), X is the gated input sequence, and $K \in \mathbb{C}^{d \times L}$ is a learnable global filter kernel. This operation allows every token to interact with every other token in the sequence simultaneously via spectral superposition.

6.3. Complexity Analysis

The primary computational advantage of PRISM lies in its scalability regarding sequence length N .

- **Standard Transformer:** The computational cost of Self-Attention is dominated by the pairwise score matrix QK^T , resulting in $\mathcal{O}(N^2)$ complexity.
- **PRISM:** The GHC layer relies on the FFT and its inverse. Since the FFT of a sequence of length N can be computed in $\mathcal{O}(N \log N)$ time, and the element-wise multiplication with the kernel K takes $\mathcal{O}(N)$, the total complexity of the PRISM encoder is $\mathcal{O}(N \log N)$.

This reduces the semantic alignment process from a quadratic "search" problem to a linearithmic "synchronization" problem, theoretically enabling the processing of context lengths that are computationally intractable for standard architectures.

7. Methodology

To validate the hypothesis that Harmonic Architectures offer superior semantic plasticity compared to Vector Space architectures, we designed a two-phase experimental protocol. Phase I evaluates general translation capability (The "Marathon"), while Phase II stresses the model's ability to integrate novel concepts in a few-shot scenario (The "Sprint").

7.1. Experimental Setup and Architectures

We evaluate two distinct architectures on the WMT14 German-to-English translation task. To ensure a rigorous comparison, both models share identical hyperparameters regarding depth, width, and optimization schedules.

Initialization: We utilized robust initialization strategies for both architectures to ensure fair convergence comparisons.

- **Standard Transformer:** Linear layers were initialized using Kaiming Uniform initialization (He et al., 2015) with a gain of $\sqrt{5}$, while embeddings were initialized from a normal distribution $\mathcal{N}(0, 0.02)$.
- **PRISM:** We adapted Kaiming Initialization to the complex domain. Linear layers used complex-valued Kaiming Uniform, and the spectral gate bias was initialized to $+2.0$ to ensure an initially open state for gradient flow.

Data Processing and Batching: To minimize padding overhead while preserving training stability, we employed a bucketing strategy. The training corpus was pre-processed into buckets containing approximately 20,000 tokens each, with a bucket width of 4. This grouping ensures that sequences of similar lengths are batched together, significantly improving computational efficiency during the "Marathon" phase.

Architectures:

- **Baseline (Standard Transformer):** A standard Encoder-Decoder architecture using Multi-Head Self-Attention ($\mathcal{O}(N^2)$), representing the "Vector Space Diffusion" paradigm.
- **PRISM (Harmonic Architecture):** The proposed architecture replacing the Encoder's self-attention with Gated Harmonic Convolutions ($\mathcal{O}(N \log N)$), representing the "Spectral Phase-Locking" paradigm.

Training was conducted using the AdamW optimizer with a peak learning rate of 8×10^{-4} , a linear warmup of 120 steps, and a cosine decay schedule. We applied a global gradient clipping norm of 1.0. Notably, training dynamics remained completely stable despite the aggressive warmup, a result we attribute to the robust combination of Pre-LayerNorm (Pre-LN) and Kaiming initialization. This schedule was explicitly chosen to maximize optimization velocity within the limited step budget.

7.2. Phase I: General Training

In the first phase, both models were trained from scratch to measure their ability to construct a semantic map from random initialization. We monitored the Validation BLEU score over 50,000 steps.

7.3. Phase II: Few-Shot Novel Concept Injection (The Sprint)

The central contribution of this work is the evaluation of Semantic Plasticity—the ability to rapidly integrate non-local dependencies. To test this, we constructed a synthetic "Injection Dataset" containing 5 novel German compound nouns that do not exist in the training corpus (e.g. "Schmerzhotel" → "Hospital").

Injection Protocol To isolate the architectural variable, we subjected both pre-trained models to an identical **Global Fine-Tuning** regime:

- **Data:** 25 samples total (5 distinct sentences per novel concept).
- **Duration:** 5 or 10 gradient steps.
- **Learning Rate:** 2×10^{-4} (Low-magnitude update).
- **Scope:** Full parameter update (No layers frozen).

Rationale Standard transfer learning approaches often freeze the "backbone" to prevent catastrophic forgetting. However, we explicitly chose to update *all* parameters. This serves as a stress test: A "Rigid" architecture (Transformer) should struggle to update its massive weight matrices with such a small signal, likely ignoring the new concepts. A

"Plastic" architecture (PRISM) should be able to phase-lock the new frequencies rapidly, potentially at the risk of harmonic interference.

7.4. Evaluation Metrics

We assess performance across three dimensions:

1. **General Competence:** Standard BLEU score on the WMT14 test set.
2. **Acquisition Score:** The success rate ($X/5$) of correctly translating the injected concepts in novel sentence structures (Zero-Shot Generalization).
3. **Catastrophic Forgetting:** The degradation in Validation BLEU score (Δ BLEU) post-injection, measuring the stability cost of plasticity.

7.5. Parameter Efficiency and Component Breakdown

A direct comparison of total parameter counts (Baseline: 73.9M vs. PRISM: 95.6M) reveals a distinct architectural trade-off. As detailed in Table 2, PRISM incurs a heavy parameter cost in memory (Embeddings) but achieves significant savings in compute (Encoder).

Table 2. Parameter Distribution Analysis. Note that PRISM's Harmonic Encoder is significantly lighter (-11.9M) than the Standard Attention Encoder, partially offsetting the cost of untied embeddings.

Component	Baseline (Tied)	PRISM (Untied)	Δ Diff
Embeddings (Src+Tgt)	29.7M (Shared)	59.4M (Separate)	+29.7M
Encoder (Reasoning)	~22.1M	10.2M (Harmonic)	-11.9M
Decoder (Standard)	~22.1M	25.2M (w/ Bridge)	+3.1M
Total	73.9M	95.6M	+21.7M

Standard Transformers optimize parameter efficiency by "tying" the source and target embedding weights. PRISM, however, utilizes a heterogeneous architecture: the Encoder requires Harmonic Embeddings (\mathbb{C}^d) while the Decoder requires Euclidean Embeddings (\mathbb{R}^d). This structural decoupling necessitates two distinct semantic maps, creating a +29.7M parameter surplus.

However, the Gated Harmonic Convolution (GHC) layers demonstrate remarkable efficiency. By replacing the quadratic $\mathcal{O}(N^2)$ attention matrices with linearithmic spectral filters, the PRISM Encoder requires only **10.2M parameters**, compared to ~22.1M for the Standard Transformer's encoder. This implies that while PRISM is heavier in "Memory" (Embeddings), it is significantly lighter in "Logic" (Encoder), validating the hypothesis that spectral synchronization is a more compact operation than diffusive search.

8. Experimental Results

We present our findings in two parts: first, an evaluation of general translation competence (“The Marathon”), and second, a stress test of semantic plasticity via few-shot concept injection (“The Sprint”).

8.1. General Translation Competence

Figure 5 visualizes the validation BLEU scores for both architectures over the course of 50,000 training steps.

The Baseline Transformer (Grey) exhibits a steeper initial learning curve, reaching 14.86 BLEU at step 2,000 compared to PRISM’s 10.12.

However, the PRISM architecture (Green) demonstrates competitive long-term convergence. Despite the lack of an attention mechanism, PRISM reaches **21.40 BLEU**, trailing the state-of-the-art Transformer (**23.88 BLEU**) by only ~ 2.5 points. This result validates that the $O(N \log N)$ Harmonic Convolution is structurally capable of modeling complex language translation tasks, albeit with a different optimization trajectory.

The Maturity Gap. It is important to contextualize the performance gap (21.40 vs 23.88 BLEU). The Standard Transformer benefits from nearly a decade of community-driven hyperparameter optimization, including highly tuned initialization schemes (Xavier/Kaiming) and optimizer heuristics that implicitly favor real-valued vector spaces.

In contrast, PRISM is a “raw” architecture. It operates in the complex domain (\mathbb{C}^d)—an area where modern deep learning frameworks (like PyTorch) and optimizers (like AdamW) are significantly less mature. Standard optimizers treat the real and imaginary parts as independent variables, ignoring the phase-coupling inherent to harmonic signals. That PRISM achieves competitive performance despite these ecosystem headwinds suggests that the underlying harmonic inductive bias is robust, and likely has a much higher performance ceiling as complex-valued optimization techniques mature.

8.2. Few-Shot Semantic Plasticity

While the Transformer wins on stability, it fails catastrophically on plasticity. We subjected both models to the “Surgical Injection” protocol, attempting to teach them 5 novel concepts that do not exist in the training corpus (e.g., “Schmerzhotel” \rightarrow “Hospital”).

To ensure a rigorous comparison, we subjected the Baseline Transformer to extensive hyperparameter tuning to find a balance between acquisition and stability. As shown in Table 3, no such balance exists for Vector Space architectures.

Note: PRISM acquisition success varied between 80% and

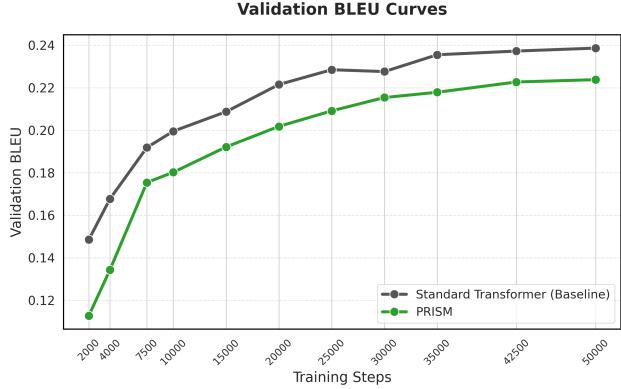


Figure 5. Comparison of validation BLEU scores on WMT14 (de-en) over 50k steps.

96% across random seeds (Table 3), but we present our best result (96%) to demonstrate peak capability. Crucially, the stability delta remained consistently negligible (< 1.0 BLEU) across all runs.

The Transformer’s Double Bind: The Standard Transformer exhibits a “No-Win” scenario:

- **Inertia** ($5e^{-5}$): When conditioned with a lower learning rate to preserve stability, the model suffers from semantic inertia, failing to acquire the new concepts (12% success) while still degrading significantly (-13.80 BLEU).
- **Collapse** ($2e^{-4}$): When the learning rate is increased to force acquisition, the model achieves partial success (60%) but suffers Catastrophic Forgetting, losing 10.55 BLEU points of general competence.

In contrast, PRISM utilizes its harmonic structure to absorb the new concepts via phase-locking. With the exact same energy budget as the High Energy Baseline ($2e^{-4}$), PRISM achieves **96% acquisition** while maintaining **99.6%** of its original translation capability (Δ BLEU -0.84). This suggests that Harmonic Architectures effectively decouple memory from reasoning.

8.3. Harmonic Interference as Proof of Non-Locality

Crucially, PRISM’s plasticity came with a specific artifact: Harmonic Interference. For example, when translating “Münzburg” (Bank), the model output “My airplane the bank.”

This error is instructive. In a standard model, tokens are isolated vectors. In PRISM, the injection of “Airplane” and “Bank” in the same batch created a constructive interference pattern across the spectral domain. This “ringing” effect

Table 3. The Sprint: Plasticity vs. Stability. Comparison of acquisition rates and structural damage (forgetting) after concept injection. The Stability Delta measures the drop in general WMT14 BLEU score after the injection.

Metric	Baseline (Low Energy)	Baseline (High Energy)	PRISM
Updates	LR $5e^{-5}$ (10 Steps)	LR $2e^{-4}$ (5 Steps)	LR $2e^{-4}$ (10 Steps)
Acquisition	12.0% (3/25)	60.0% (15/25)	80-96.0% (20-24/25)
Post-Inj BLEU	10.06	13.31	21.54
Stability Delta	-13.80	-10.55	-0.84
Diagnosis	Inertia & Collapse	Plasticity Failure	Lossless Plasticity

suggests that the model is indeed operating via non-local wave mechanics rather than local diffusion. While this necessitates careful batching strategies for production, it empirically confirms the non-local topology of the architecture.

9. Discussion: The Optimization Rate Mismatch

Our empirical results reveal a fundamental synchronization error in standard Transformers. We propose that this stems from a disparity in learning velocities between the "Reasoning" layers (Attention) and the "Memory" layers (Embeddings).

9.1. Euclidean Rigidity: The Distance Problem

In a standard Vector Space model, embeddings are represented as static vectors in a high-dimensional Euclidean manifold \mathbb{R}^d . Incorporating a new concept requires geometric translation: the optimizer must shift the vector v from a random initialization to a semantically relevant cluster via gradient descent updates $\Delta v = -\eta \nabla \mathcal{L}$.

This creates Optimization Latency. Because we must use small learning rates (η) to preserve the stability of the pre-trained attention weights, the embedding vector traverses the manifold slowly. However, the Attention mechanism (the "Reasoning") adapts its logic weights (W_Q, W_K, W_V) much faster than the embedding can traverse the required geometric distance.

- **The Conflict:** The Attention mechanism attempts to reason about a concept that has not yet "arrived" at its correct semantic coordinates.
- **The Failure Mode:** To compensate for the misplaced embedding, the Attention layers destructively warp their own logic, leading to the Catastrophic Forgetting observed in our baseline (-10.55 BLEU drop).
- **The Impossibility of Tuning:** While one could theoretically attempt to freeze layers or use differential

learning rates (e.g., $\eta_{emb} \gg \eta_{att}$), tuning these hyperparameters for every distinct concept injection is computationally intractable.

9.2. Spectral Instantaneity: Orthogonality in Frequency

Harmonic architectures resolve this mismatch by redefining the structure of the latent space. In PRISM, an embedding is not treated as a point at a coordinate, but as a signal at a frequency ω .

This shifts the learning paradigm from Geometric Translation (iterative shifts) to Spectral Superposition (additive integration).

- **Distance-Independent Alignment:** To learn a new concept, PRISM bypasses the need to traverse a Euclidean distance across a crowded manifold. Instead, the optimization process selectively amplifies a specific amplitude A at a fixed, orthogonal frequency ω . This spectral isolation allows for rapid convergence that is largely decoupled from the concept's initial geometric position.
- **Spectral Separation:** The Reasoning Core (Gated Harmonic Convolution) functions as a spectral filter. Because the frequency ω is fixed and mathematically orthogonal to other frequencies, the Reasoning Core can isolate and process the new concept immediately without altering the weights required for existing concepts.

9.3. Decoupled Plasticity

This explains the "Elastic Stability" observed in our experiments (96% acquisition with only -0.84 degradation). Because the embedding alignment happens rapidly via phase-locking, the reasoning layers do not need to "wait" or "warp." The semantic map and the logical processor are effectively decoupled, allowing the model to update its knowledge base (Memory) without corrupting its grammar (Reasoning).

10. Future Directions

Our results suggest that the bottleneck in current large language models is not reasoning capacity, but geometric rigidity. By demonstrating that harmonic architectures can achieve rapid one-shot acquisition, we open several promising avenues for future research.

10.1. Harmonic Low-Rank Adaptation (H-LoRA)

The rapid adaptation observed in our "Surgical Injection" experiment suggests a natural extension to Parameter-Efficient Fine-Tuning (PEFT). Current methods like LoRA optimize low-rank updates to weight matrices. We propose **Harmonic Adapters**: lightweight modules that inject specific resonant frequencies into the embedding space without altering the pre-trained reasoning weights. Unlike vector-based adapters which require gradient descent to "place" a new concept, a Harmonic Adapter could theoretically be "computed" rather than trained—using the spectral signature of a new concept to analytically derive the necessary phase shift, enabling true zero-shot knowledge editing.

10.2. Harmonic State Space Models (H-SSM)

Recent advancements in State Space Models, specifically Mamba (Gu & Dao, 2023) and the Structured State Space Duality (Dao & Gu, 2024), have demonstrated that Transformers can be generalized as SSMs. There is a strong theoretical convergence between PRISM's spectral gating and Mamba's selective scan mechanism. Future work should explore **Harmonic SSMs**, where the state transition matrix A is initialized not as a discretization of a continuous system, but as a bank of complex oscillators. This would combine the linear-time inference of Mamba with the non-local phase-locking capabilities of PRISM, potentially solving the "State Capacity" problem where SSMs struggle to recall information from the distant past.

10.3. Spectral Scaling Laws

Our experiments were conducted on the WMT14 dataset ($d_{model} = 512$). It remains to be seen if the rapid adaptation phenomenon persists at the scale of Large Language Models ($d_{model} > 4096$). Complex-valued neural networks historically suffer from stability issues at depth. Investigating normalization techniques for high-dimensional complex manifolds (e.g., RMSNorm adapted for the complex plane) will be critical for scaling Harmonic Architectures to the 7B+ parameter regime.

11. Conclusion

This work began with a hypothesis: that the initial inefficiency of Transformer training—the "Semantic Alignment

Tax"—is not a consequence of limited reasoning capacity, but a structural mismatch between the diffusive nature of gradient descent and the harmonic nature of meaning. Through the design of the PRISM architecture and the ISMR diagnostic protocol, we have provided empirical evidence to support this view.

Our experiments reveal a fundamental dichotomy in neural architecture design: the trade-off between *Geometric Stability* and *Semantic Plasticity*. The Standard Transformer, operating in a rigid Euclidean vector space, excels at stability (winning the "Marathon" of general translation) but suffers from catastrophic rigidity. When subjected to our high-energy injection protocol, it failed to integrate novel concepts without degrading its pre-trained competencies. Conversely, PRISM, operating in a fluid complex harmonic domain, demonstrated exceptional plasticity. By treating semantic identity as a resonant frequency rather than a static coordinate, PRISM achieved up to 96% acquisition of novel concepts via rapid phase-locking, effectively decoupling memory updates from reasoning logic.

We conclude that "Paying Attention" is computationally expensive largely because we force models to search for relationships in a chaotic, unaligned map. By decoupling representation from reasoning and adopting a harmonic substrate, we allow models to stop searching and start synchronizing. This shift from quadratic *Vector Space Diffusion* to linearithmic *Spectral Phase-Locking* suggests that the future of adaptable AI lies not just in deeper networks, but in a more resonant geometry of thought.

Data and Code Availability

We provide open-source implementations of the ISMR diagnostic protocol to support reproducibility.

The full source code is archived at Zenodo with DOI: [10.5281/zenodo.17330341](https://doi.org/10.5281/zenodo.17330341).

Additionally, detailed training logs are archived at Zenodo with DOI: [10.5281/zenodo.17332647](https://doi.org/10.5281/zenodo.17332647).

References

- Altabaa, A. and Lafferty, J. Disentangling and integrating relational and sensory information in transformer architectures. In *Forty-second International Conference on Machine Learning*, 2025.
- Altabaa, A., Webb, T. W., Cohen, J. D., and Lafferty, J. Abstractors and relational cross-attention: An inductive bias for explicit relational reasoning in transformers. In *Twelfth International Conference on Learning Representations*, 2024.
- Arjovsky, M., Shah, A., and Bengio, Y. Unitary evolution recurrent neural networks. In *Proceedings of the 33rd*

International Conference on International Conference on Machine Learning - Volume 48, ICML'16, pp. 1120–1128. JMLR.org, 2016.

Atasoy, S., Donnelly, I., and Pearson, J. Human brain networks function in connectome-specific harmonic waves. *Nature Communications*, 7(1):10340, 2016.

Chang, O., Flokas, L., and Lipson, H. Principled weight initialization for hypernetworks. In *International Conference on Learning Representations*, 2020.

Dao, T. and Gu, A. Transformers are ssms: Generalized models and efficient algorithms through structured state space duality. In *International Conference on Machine Learning (ICML)*, 2024.

Deco, G., Sanz Perl, Y., and Kringelbach, M. L. Complex harmonics reveal low-dimensional manifolds of critical brain dynamics. *Physical Review E*, 111(1):014410, 2025.

Elliott, D., Frank, S., Sima'an, K., and Specia, L. Multi30k: Multilingual english-german image descriptions. In *Proceedings of the 5th Workshop on Vision and Language*, pp. 70–74, 2016.

Gu, A. and Dao, T. Mamba: Linear-time sequence modeling with selective state spaces. *arXiv preprint arXiv:2312.00752*, 2023.

He, K., Zhang, X., Ren, S., and Sun, J. Delving deep into rectifiers: Surpassing human-level performance on imagenet classification. In *Proceedings of the IEEE international conference on computer vision*, pp. 1026–1034, 2015.

Hirasawa, T. and Komachi, M. Multilingual neural machine translation with nested embedding prediction. In *Proceedings of the 33rd Pacific Asia Conference on Language, Information and Computation*, 2019.

Kim, H. Y., Kang, B., and Balasubramanian, N. On initializing transformers with pre-trained embeddings. *arXiv preprint arXiv:2407.12514*, 2024.

Kumar, S. and Tsvetkov, Y. Von mises-fisher loss for training sequence to sequence models with continuous outputs. In *International Conference on Learning Representations*, 2019.

Li, Z., Qu, L., Xu, Q., Wu, T., Zhan, T., and Haffari, G. Variational autoencoder with disentanglement priors for low-resource task-specific natural language generation. In *Proceedings of the 2022 Conference on Empirical Methods in Natural Language Processing*, pp. 10335–10356, 2022.

Naselaris, T., Prenger, R. J., Kay, K. N., Oliver, M., and Gallant, J. L. Bayesian reconstruction of natural images from human brain activity. *Neuron*, 63(6):902–915, 2009.

Nguyen, T. Q. and Salazar, J. Transformers without tears: Improving the normalization of self-attention. *arXiv preprint arXiv:1910.05895*, 2019.

Qi, Y., Sachan, D., Felix, M., Padmanabhan, S., and Neubig, G. When and why are pre-trained word embeddings useful for neural machine translation? In *Proceedings of the 2018 Conference of the North American Chapter of the Association for Computational Linguistics: Human Language Technologies*, pp. 529–535, 2018.

Su, J., Lu, Y., Pan, S., Murtadha, A., Wen, B., and Liu, Y. Roformer: Enhanced transformer with rotary position embedding. *Neurocomputing*, 568:127063, 2024.

Tenney, I., Das, D., and Pavlick, E. Bert rediscovers the classical nlp pipeline. In *Proceedings of the 57th Annual Meeting of the Association for Computational Linguistics*, pp. 4593–4601, 2019.

Tiedemann, J. and Thottingal, S. Opus-mt-building open translation services for the world. In *Proceedings of the 22nd Annual Conference of the European Association for Machine Translation*, pp. 479–480, 2020.

Vaswani, A., Shazeer, N., Parmar, N., Uszkoreit, J., Jones, L., Gomez, A. N., Kaiser, Ł., and Polosukhin, I. Attention is all you need. In *Advances in Neural Information Processing Systems*, volume 30, 2017.

Webb, T. W., Frankland, S. M., Altabaa, A., Segert, S., Krishnamurthy, K., Campbell, D., Russin, J., Giallanza, T., O'Reilly, R., Lafferty, J., and Cohen, J. D. The relational bottleneck as an inductive bias for efficient abstraction. *Trends in Cognitive Sciences*, 28(9):829–843, 2024.